Chapter 4 Field Survey and Numerical Simulation on the 2004 Off-Sumatra Earthquake and Tsunami in Thailand

4.1 Introduction

On December 26, 2004 at 07:59 am (UTC 00:59 am, JST 09:59 am), a giant earthquake occurred off the west coast of northern Sumatra, Indonesia. Its epicenter is shown in Fig. 4.1. Fig. 4.2 shows that the seismic activity in this region is very high as the Pacific Rim.

Its magnitude was reported by some institutes as shown in Table 4.1. The West Coast Alaska Tsunami Warning Center and the Pacific Tsunami Warning Center issued magnitude 8.0 warnings within fifteen minutes of the earthquake. The magnitude 9.0 which is well-known nowadays was reported nineteen hours later. These revised magnitudes, however, do not mean the centers made mistakes, but indicate the difficulty in analyzing such a giant earthquake in such a short time, even for leading seismologists. This was the fourth largest earthquake in the world since 1900, see Fig. 4.3 and Table 4.2. Another earthquake which occurred in this region three months later was the seventh largest event.

The giant earthquake generated a huge tsunami which was the third largest since 1900, as shown in Table 4.3. This tsunami hit many countries in the Indian Ocean. With the exception of Indonesia, the Andaman Islands and Nicobar Islands, the tsunami, not the earthquake, caused all of the extensive damage (see Fig. 4.4.). This was the greatest tsunami disaster in history.

The tsunami hit the southeast coast of Thailand, which was about 500 km from the epicenter. Because the area has world famous resorts like Phuket Island and the tsunami hit the coast at around high tide (Fig. 4.5), there was a dreadful tragedy. 5,400 people were killed and 3,100 people reported missing due to the tsunami in Thailand. To study this disaster, a field survey was carried out from December 30, 2004 to January 3, 2005 along the southeast coast of Thailand. Further, a numerical simulation was conducted to investigate the source mechanism of the tsunami. In this chapter, those results are reported.

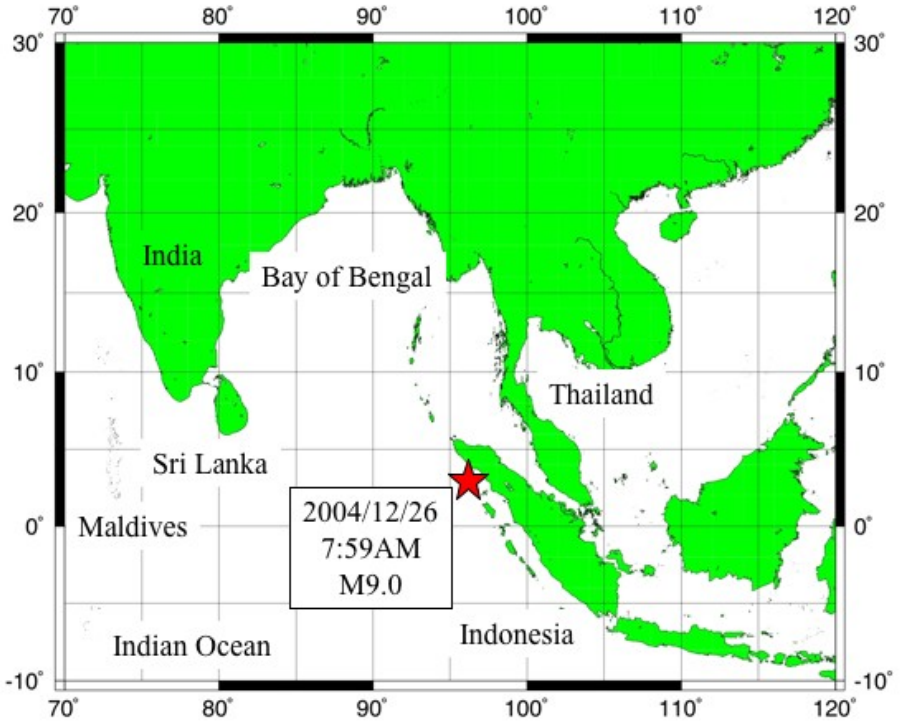

Fig. 4.1 The epicenter of the 2004 Sumatra Earthquake

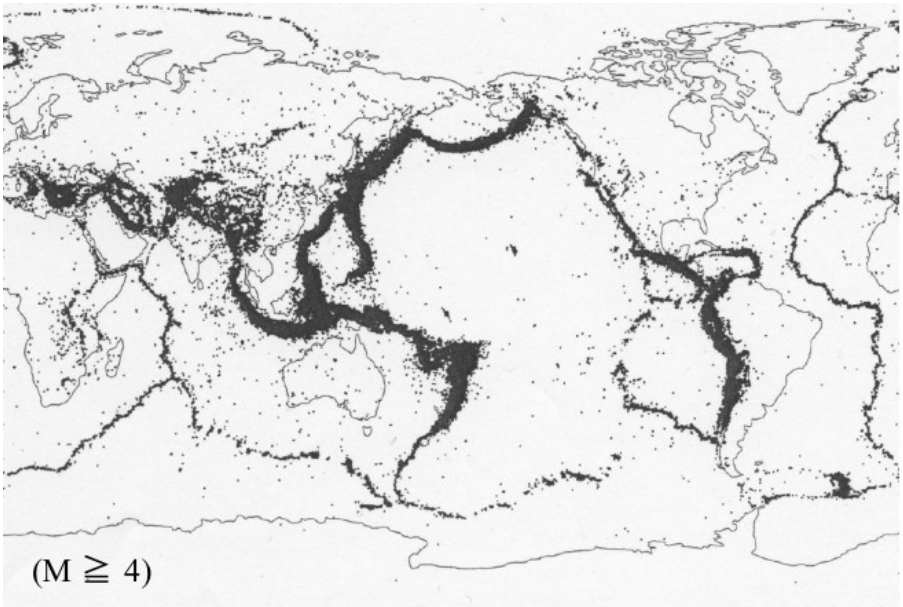

Fig. 4.2 Seismic activity in the world from 1978 to 2000 (Utsu, 2001)

Table 4.1 A history of reported magnitude of the earthquake

Institute	Magnitude *1	Issued time (UTC) *2	Time after the event *3
WCATWC	M 8.0	12/26/2004 01:14	00:15
PTWC	M 8.0	12/26/2004 01:14	00:15
PTWC	M 8.5	12/26/2004 02:04	01:05
WCATWC	M 8.5	12/26/2004 02:09	01:10
USGS	M 8.5	12/26/2004 02:17	01:18
USGS	Mw 8.2	12/26/2004 02:23	01:24
Harvard Univ.	Mw 8.9	12/26/2004 05:26	04:27
Harvard Univ.	Mw 9.0	12/26/2004 20:02	19:03
WCATWC	M 9.0	12/27/2004 15:34	36:35
PTWC	M 9.0	12/27/2004 15:35	36:36

*1 "M" means that the type of magnitude was not shown in the e-mail.

*2 Where no issued time was shown in the e-mail, the posted time informed by the institute's SMTP server is used.

*3The origin time of the earthquake is assumed to be 12/26/2004 00:59 UTC by USGS.

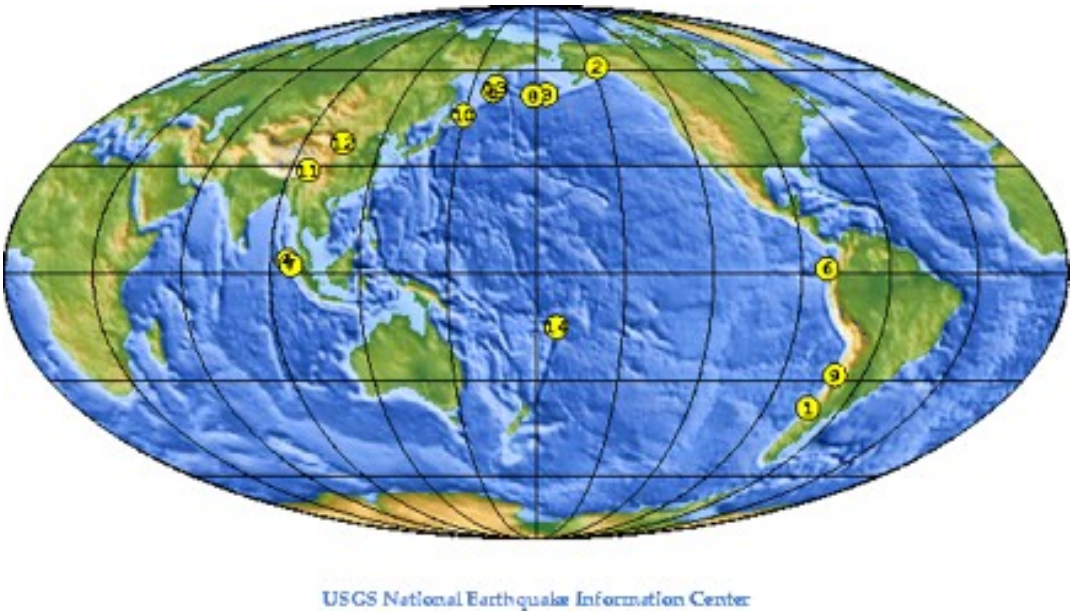

Fig. 4.3 Largest earthquakes in the world since 1900 (USGS, 2005)

Table 4.2 Largest earthquakes in the world since 1900 (USGS, 2005)

	Location	Date UTC	Magnitude	Coordinates	
1	Chile	1960 05 22	9.5	38.24 S	73.05 W
2	Prince William Sound, Alaska	1964 03 28	9.2	61.02 N	147.65 W
3	Andreanof Islands, Alaska	1957 03 09	9.1	51.56 N	175.39 W
4	Off the West Coast of Northern Sumatra	2004 12 26	9.0	3.30 N	95.78 E
5	Kamchatka	1952 11 04	9.0	52.76 N	160.06 E
6	Off the Coast of Ecuador	1906 01 31	8.8	1.0 N	81.5 W
7	Northern Sumatra, Indonesia	2005 03 28	8.7	2.08 N	97.01 E
7	Northern Sumatra, Indonesia	2005 03 28	8.7	2.08 N	97.01 E
13	Kamchatka	1923 02 03	8.5	54.0 N	161.0 E
14	Tonga	1917 06 26	8.5	15.0 S	173.0 W

Table 4.3 Largest tsunamis in the world since 1900 (Abe, 2005)

	Earthquake	Date UTC	Mt
1	Chile	1960 05 22	9.4
2	Aleutians	1946 04 01	9.3
3	Sumatra, Indonesia	2004 12 26	9.1
4	Alaska	1964 03 28	9.1
5	Kamchatka	1952 11 04	9.0
5	Aleutians	1957 03 09	9.0

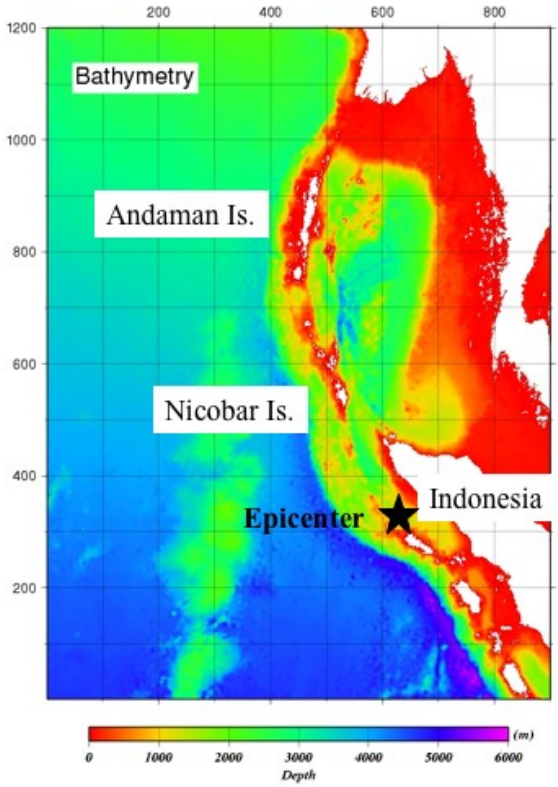

Fig. 4.4 Bathymetry

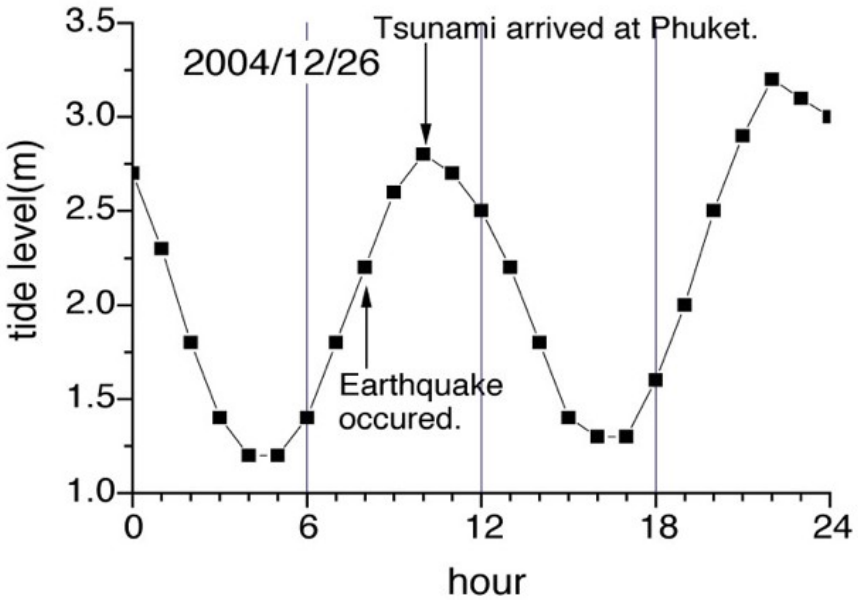

Fig. 4.5 The tidal change and the tsunami arrival time at Phuket

4.2 Field Survey

4.2.1 Period and Team Members of Field Survey

The survey was conducted from December 30, 2004 to January 3, 2005. In the afternoon of January 3, we hold a press conference and reported the preliminary results of our field survey at the Thai government's request. Our field survey team consisted of the following members:

[JAPAN]

Hideo Matsutomi (Akita University) Survey team leader
Tomoyuki Takahashi (Akita University)
Tetsuya Hiraishi (Port and Airport Research Institute)
Masafumi Matsuyama (Central Research Institute of the Electric Power Industry)
Kenji Harada (Disaster Reduction and Human Renovation Institution)
Sittichai Nakusakul (Yokohama National University)

[THAILAND]

Seree Supartid (Ransit University)
Mongkonkorn Srivichai (Rangsit University)
Suchart Limkatanyu (Prince of Songkhla University)
Danupon Tonnayopas (Prince of Songkhla University)
Pruittikorn Smithmaitrie (Prince of Songkhla University)
Jareerat Sakulrat (Prince of Songkhla University)
Wattana Kanbua (Thai Meteorological Department)
Chaitawat Siwabowon (Ministry of Interior, Thai)
Sittiporn Phetdee (Ministry of Interior, Thai)
Warlsatha Janchoowong (Ministry of Interior, Thai)
Suchaya Suttiwanakul (Ministry of Interior, Thai)

Photo 4.1 Field Service press conference in Phuket

4.2.2 Objective of Field Survey

The general objective of the field survey on the disaster is to determine the damage caused and to study the factors involved. The magnitude of the damage is a result of a balance between factors on the side of the disaster and factors on the human side. In a tsunami disaster, the former factors imply tsunami height, velocity, hydraulic power, etc. and the latter factors imply preparedness, countermeasures, education, evacuation, etc. Many field surveys are desired to investigate factors on both sides. Our field survey, however, was carried out just 4 days after the disaster, and it was during the phase of rescue, relief and rehabilitation operations. We really needed to interview the authorities concerned and collect official documents to study the factors on the human side, but we were afraid of hindering releif operations. Further, there was a high possibility of tsunami traces disappearing immediately because of the tourist places. (When we arrived at Phuket, debris had been removed and businesses were actually open on a small damaged beach as shown in Fig. 4.2.) Therefore, we mainly investigated damage and the factors on the side of tsunami disaster as follows:

- Situation of tsunami arrival (number of waves, the largest wave, depression or elevation of the leading wave, etc.)
- Tsunami height (runup height and inundation depth)
- Inundated area
- Construction damage
- Velocity and hydraulic power
- Energy dissipation capability of vegetation

Photo 4.2 A small damaged beach in Phuket open for business on Dec. 30, four days after the disaster

4.2.3 Actual region surveyed

Our field survey was conducted along the southwest coast of Thailand, as shown in Fig. 4.6. The specific places were Khao Lak, Phuket Island and Phi Phi Islands. The investigated coastline was about 140 km long.

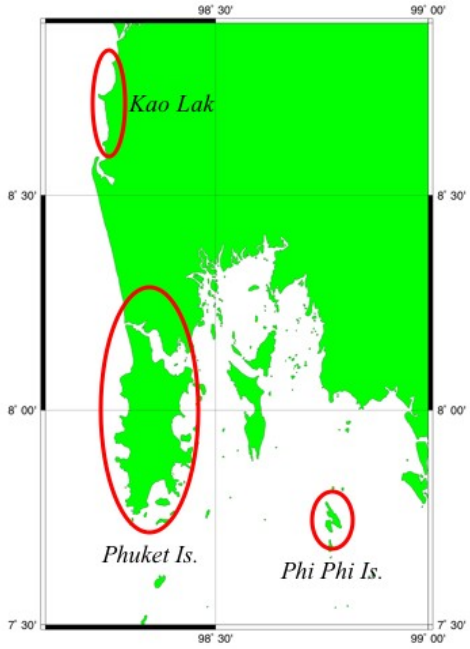

Fig. 4.6 Field survey region

4.2.4 Implementation of Field Survey

We made two or three survey groups, and investigated in the north and the south regions respectively. Transportation in the field consisted of rented cars in Khao Lak and Phuket Island, and a high-speed boat provided by the Port Authority of Thailand was used in the Phi Phi Islands.

We carried out tsunami-trace measurements and interviews with residents, as shown in Figs. 4.3 and 4.4. The tsunami traces, driftage and debris, inundation lines on walls, withered plants, etc. were probed as shown in Fig. 4.7. We took several traces to determine the typical tsunami height in the region. When a trace height was low, we confirmed it by interviewing residents. For accurate measurement of tsunami heights and distances from the shore, we used a laser distancemeter and an optic prism.

Because of the difference in tide levels between when the tsunami arrived and when our measurements were made, the measured tsunami heights were corrected by the method shown in Fig. 4.8. The tsunami arrival times were assumed to be a uniform 10:00 am local time.

Photo 4.3 The measurement of tsunami height with the laser distancemeter

Photo 4.4 Interviewing a resident

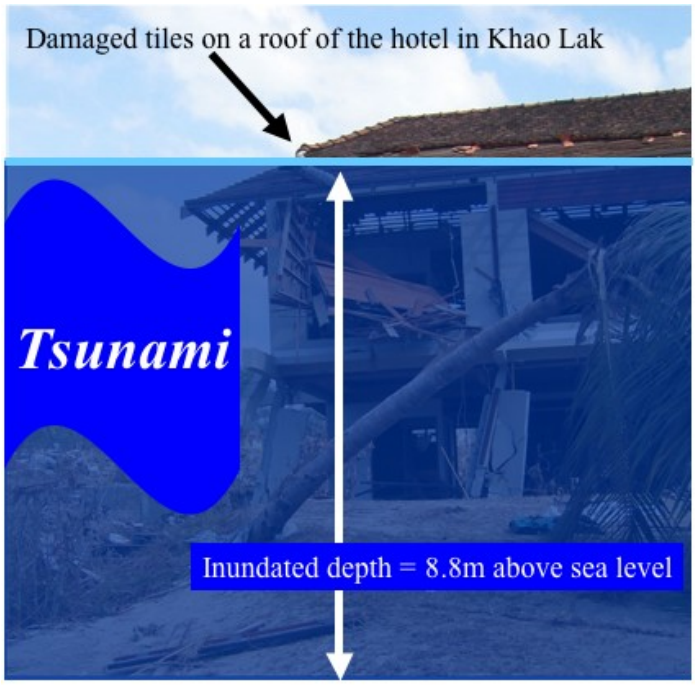

(a) Inundated depth

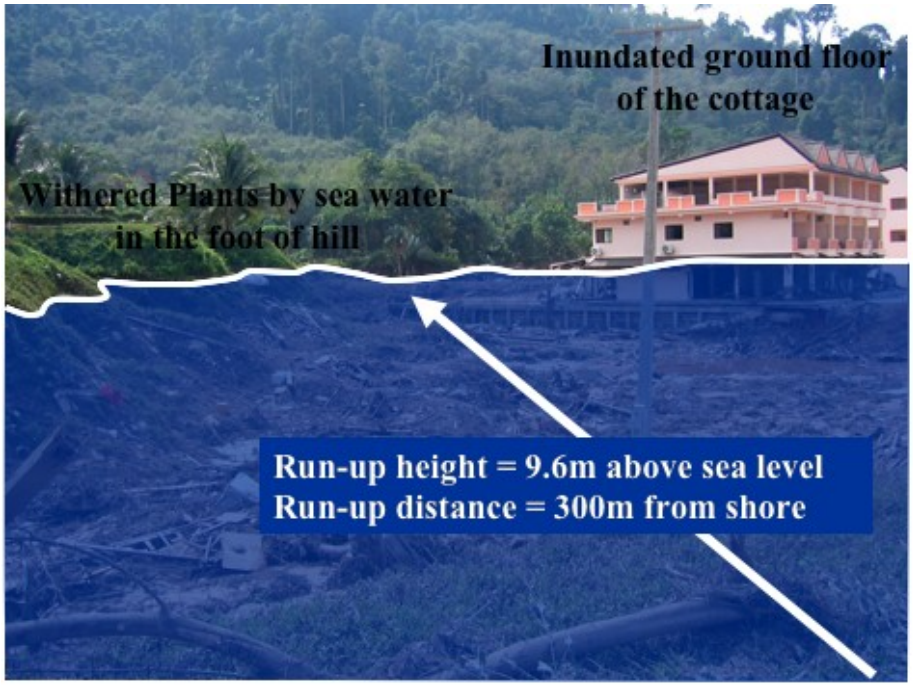

(b) Runup height and distance from shore

Fig. 4.7 Examples of tsunami trace discrimination

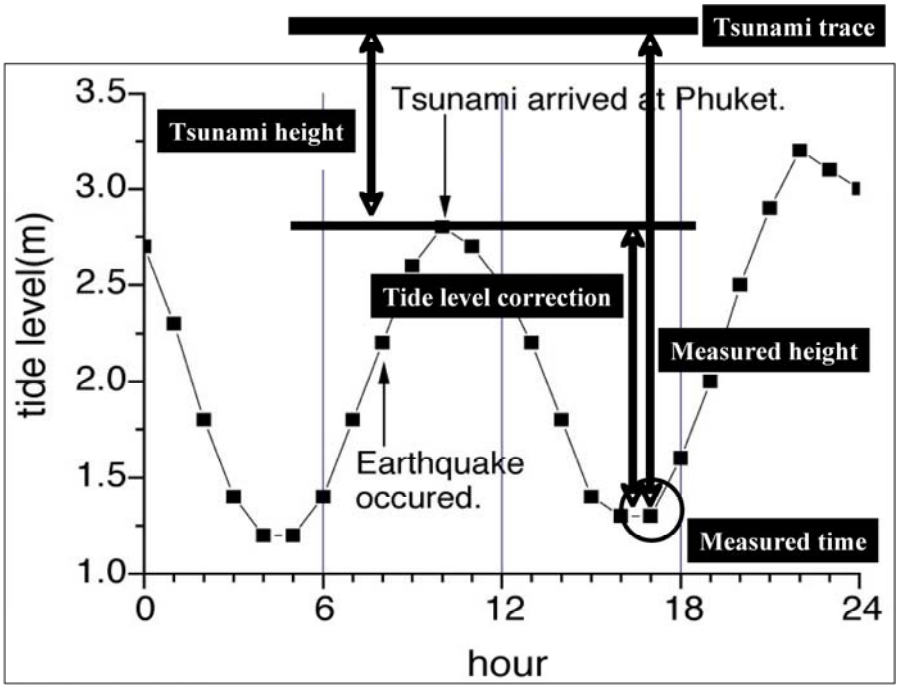

Fig. 4.8 The method of tide level correction

4.2.5 Results of the Field Survey

The measured tsunami heights in Khao Lak, Phuket Island and Phi Phi Islands are shown in Fig. 4.9. These tsunami heights have been corrected for the tide level difference described in section 4.2.4. The typical tsunami heights are 6 to 10 m in Khao Lak, 3 to 6 m along the west coast, 3 m along the south coast and 2 m along the east coast of Phuket Island, and 4 to 6 m on Phi Phi Islands.

In the following sections, the tsunamis which hit Khao Lak, Phuket Island and Phi Phi Islands are examined.

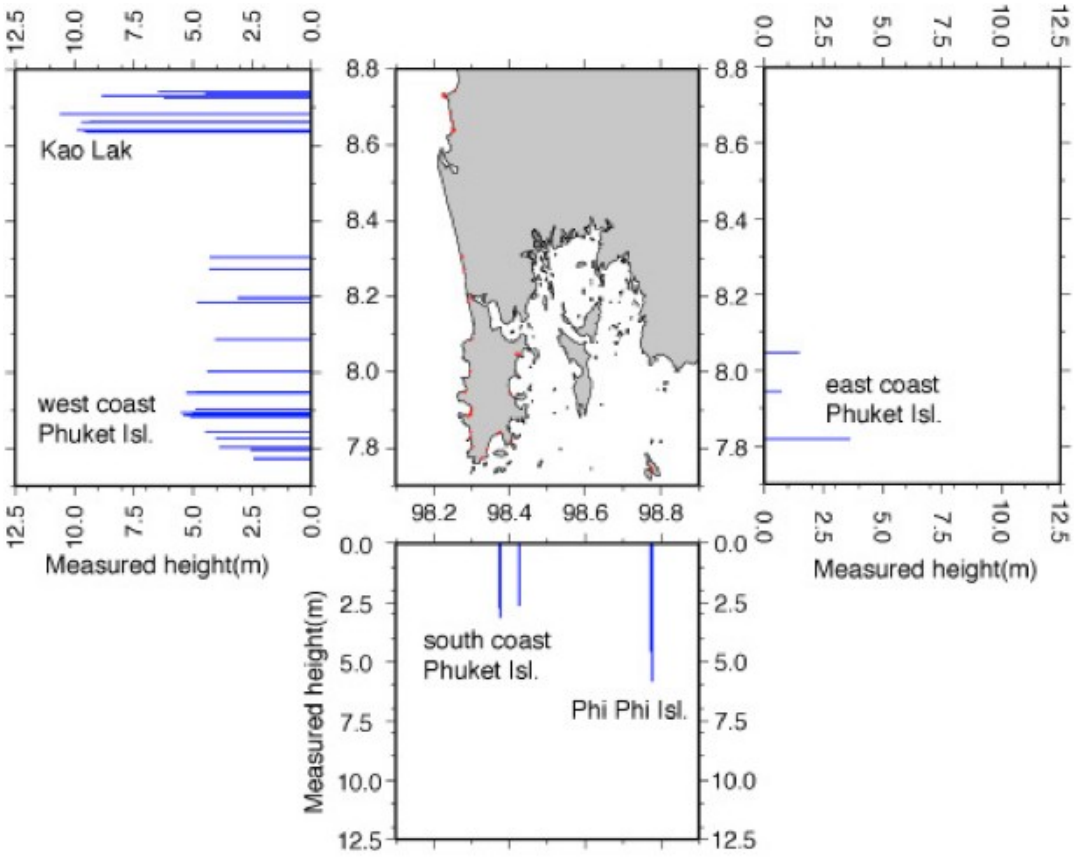

Fig. 4.9 Measured tsunami heights

(1) Khao Lak

The largest tsunami in Thailand hit this area. Some tsunami heights were higher than 10 m and the inundated depths were 4 to 7 m in the south of Khao Lak. Photo 4.5 shows that the tsunami inundated the third floor of a hotel. The tsunami heights in Khao Lak were much higher than Phuket Island. The reason for this difference seems to have been caused by the local bathymetry off Khao Lak (Suzuka, 2005) and the generation of soliton fission. Some photos and video tapes suggested there was soliton fission. Photo 4.6 and 4.7, for example, show two lines of the wave breaking at a short interval.

The velocities were 6 to 8 m/s and the drag forces were 3.8 to 6.7 tf/m^2 (3.7 to 6.6 x 10^4 Pa) in the inundated area estimated from the inundated depths in the south of Khao Lak (Matsutomi et al., 2005). This area was a new tourist place and there were many hotels and cottages. Those cottages and two-storied houses close to shore were totally destroyed. In the mid-area of the inundation, their walls and pillars were

partially flushed away. The two-storied houses consisted of floors and pillars made of reinforced concrete, and walls made of brick and mortar, but their roofs were made of tinplate and brick. Photo 4.8 was taken of the damage in the tourist place.

According to some interviews with residents, the leading wave produced an initial depression and the second wave was largest. These eyewitnesses accounts were also obtained in the west coast of Phuket Island and coincided with a record tide along the south coast of Phuket Island, as shown in the next subsection. Because there was subsidence in a east area of the tsunami source and Thailand is located eastward, the leading-depression was reasonable. The reason for the second wave being the largest seems to be a resonance effect and plural asperities of the fault plane. Fig. 4.10 by Yamanaka (2005) indicates that there were two large asperities in the north (asperity C) and the south (asperity B) areas.

The effect of energy dissipation on the tsunami due to vegetation could be confirmed in Khao Lak (Matsutomi et al., 2005). Figs. 4.9 and 4.10 show vegetation facing the sea and houses at the back of the vegetation. A distance of both places was about 150 m along the coast and the place in photo 4.10 located the north. The vegetation decreased inundated depths from 4.9 m to 4.6m.

Photo 4.5 The tsunami inundated the third floor of a hotel (left building in photo) in Khao Lak

Photo 4.6 The tsunami hits Khao Lak (BBC, 2005)

Photo 4.7 The tsunami hits Khao Lak (Amateur Asian Tsunami video Footage, 2005)

Photo 4.8 Heavily damaged hotels in Khao Lak

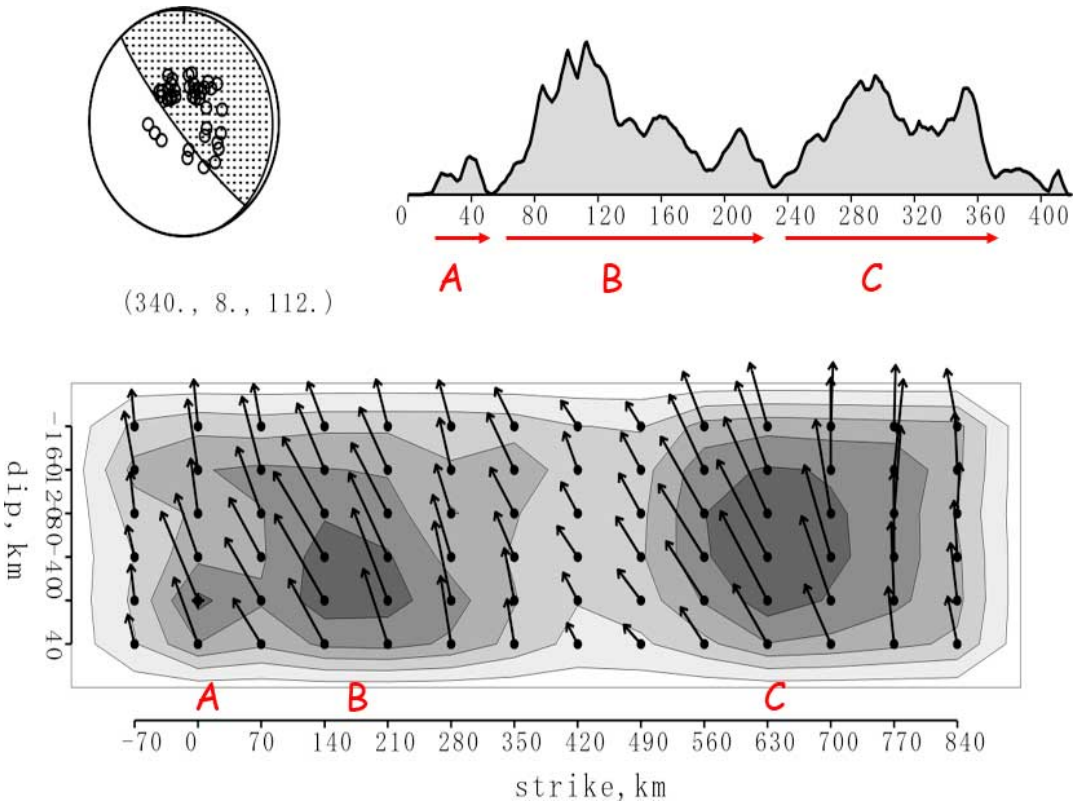

Fig. 4.10 Source rupture process of the earthquake (Yamanaka, 2005)

(a) Vegetation facing the sea

(b) A house at the back of the vegetation

Photo 4.9 An example of energy dissipation of the tsunami due to vegetation in Khao Lak

(a) Vegetation facing the sea

(b) A house behind vegetation

Photo 4.10 An example of energy dissipation of the tsunami due to vegetation in Khao Lak

(2) Phuket Island

Fig. 4.11 shows the distribution of measured tsunami heights in Phuket Island. The tsunami heights became lower from the west coast, the south coast to the east coast.

On Patong Beach on the west coast – the most popular tourist place in Phuket – the tsunami heights were 5 to 6 m and the inundated depth was about 2 m. The velocities were 3 to 4 m/s and the drag forces were 0.9 to 1.7 tf/m^2 (0.9 to 1.7 x 10^4 Pa) in the inundated area as estimated from the inundated depths (Matsutomi et al., 2005). In the event of an inundated depth of about 2 m, Japanese wooden houses would show "very heavy damage" or "substantial to heavy damage". On Patong beach, however, there were many houses built of brick and "substantial to heavy damage" was predominate, as shown in Photo 4.11.

On Karon beach on the west coast, the coastal road was built higher than the shore and it acted as a seawall, protecting a hotel which was behind it, as shown in Photo 4.12. At the southern end of Karon beach, the road was not raised and hotels were damaged.

On the east coast of Phuket Island, which was not facing the tsunami source, the tsunami height was about 2 m. In one river mouth, many boats were damaged, as shown in Photo 4.13. Fortunately, concrete bridge piers were not damaged. The tsunami propagated anticlockwise around Phuket Island, as was the case at Okushiri Island in the 1993 Hokkaido Nansei-ok Earthquake Tsunami.

According to some interviews with residents, the leading wave produced an initial depression and the second wave was the largest. This agrees with the tide record along the south coast of Phuket Island, as shown in Fig. 4.12.

Photo 4.11 The broken wall of a house built of brick at Patong beach

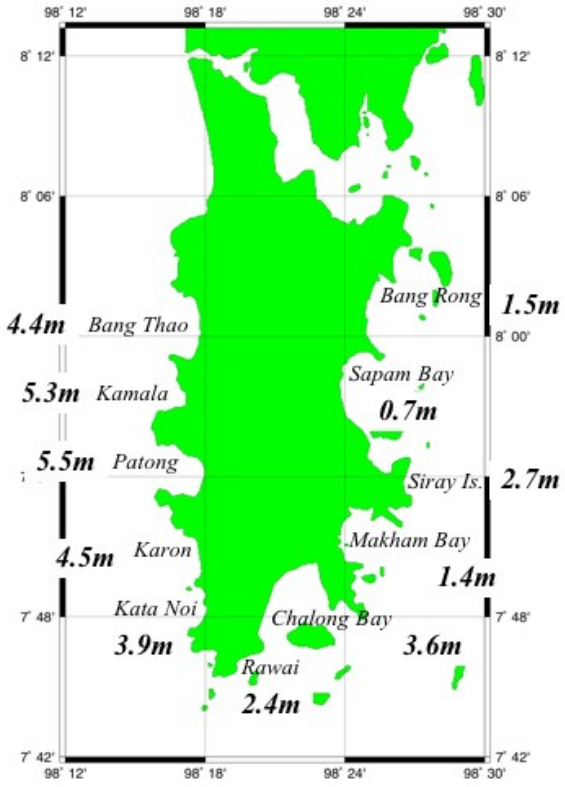

Fig. 4.11 Measured tsunami heights in Phuket Is.

Photo 4.12 Karon Beach. The high road reduced the tsunami by acting as seawall

Photo 4.13 Damaged boats in a river in the east of Phuket Is.

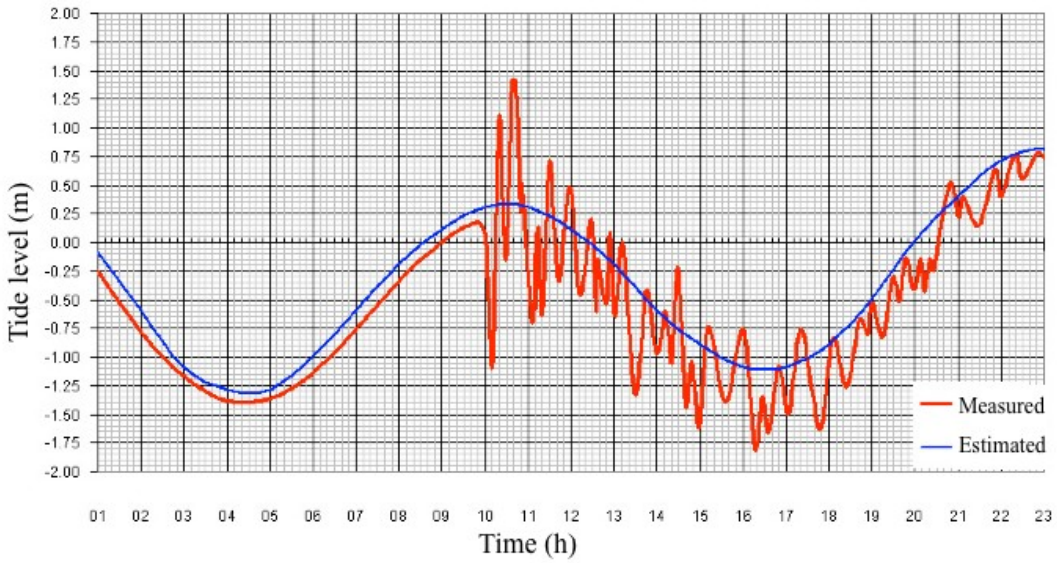

Fig. 4.12 Tide record in the south of Phuket

(3) Phi Phi Islands

Phi Phi Islands had beautiful coral reefs and were popular as scuba diving spots. The islands consist of Phi Phi Don Island and Phi Phi Le Island, as shown in Fig. 4.13. The coast of Phi Phi Le Island is bluff and nobody lived there. On Phi Phi Don Island, there were many hotels and cottages, thus the tsunami damage occurred on this island.

The shape of Phi Phi Don Island is similar to the letter "H" in shape. There are a bay on the north coast and a bay on the south coast, as shown in Photo 4.14. Photo 4.15 shows the north bay, which is shallow and had a beautiful beach. Photo 4.16 shows the south bay, which is deep and had a port.

The north bay opens to the northwest, thus it faced in the direction that the tsunami came from. The measured tsunami height on this beach was 5.8 m. On the other hand, the south bay opens to the southeast.

It faces in the opposite direction to which the tsunami was propagated. Further, Phi Phi Le Island shields the port of Phi Phi Don Island. The measured tsunami height, however, was 4.6 m in this port. It indicated that the tsunami propagated around the islands.

According to some eyewitnesses accounts, the tsunami came from the north and south, and totally washed the central area away. The ground level here was about 2 m above sea level, but there were many cottages and hotels. Therefore, the tsunami waves from the north and south destroyed this area, as shown in Photo 4.17.

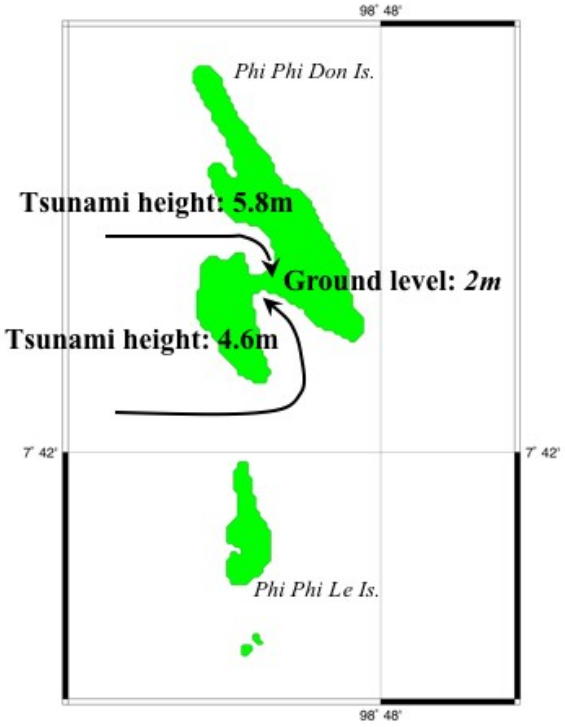

Fig. 4.13 Measured tsunami heights and ground level in Phi Phi Is.

Photo 4.14 The north and the south bays of Phi Phi Don Islands.

Photo 4.15 The north bay on Phi Phi Don Island.

Photo 4.16 The south bay which was used as a port on Phi Phi Don Island.

Photo 4.17 The central part of Phi Phi Don Island.

4.3 Numerical Simulation

4.3.1 Governing equations and numerical scheme

The numerical code is based on the linear wave theory in a polar coordinate system and no bottom friction is included. The linear wave theory is based on the depth-averaged equations of mass and momentum conservation. The conservation of mass can be written as

$$\frac{\partial \eta}{\partial t}+\frac{1}{R\cos\theta}\left[\frac{\partial M}{\partial \lambda}+\frac{\partial (N\cos\theta)}{\partial \theta}\right]=\frac{\partial \xi}{\partial t} \tag{1}$$

where η is the water-surface elevation from its equilibrium state, λ and θ are longitude and latitude, the M and N are the depth-averaged volumetric flux in the (λ, θ) horizontal directions, respectively, ξ is sea bottom deformation by crustal movement, and t time. The conservation of linear momentum in the λ and θ directions are, respectively,

$$\frac{\partial M}{\partial t}+\frac{gh}{R\cos\theta}\frac{\partial \eta}{\partial \lambda}=fN \tag{2}$$

$$\frac{\partial N}{\partial t}+\frac{gh}{R}\frac{\partial \eta}{\partial \theta}=-fM \tag{3}$$

where R is the radius of earth, f is the Coriolis coefficient ($f=2\omega\sin\theta$, ω:angular velocity), and g is gravitational acceleration. The above three equations are solved numerically for the unknowns M, N, and η, using the staggered-grid leap-frog numerical scheme (Goto and Ogawa, 1982). We used the 2 minutes digital bathymetry data published Smith and Sandwell (1997). We resampled this data and produced fine grid bathymetry data for numerical simulation. The range of the computation area is in the region of 70E-105E and 5S-23N, which is shown Fig. 4.14. The grid size consists of 3 x 3 minutes grids (area a) in the whole, and 1 x 1 minute (areas b, c), and 20 x 20 seconds (areas d, e, f) in Table 4.4.

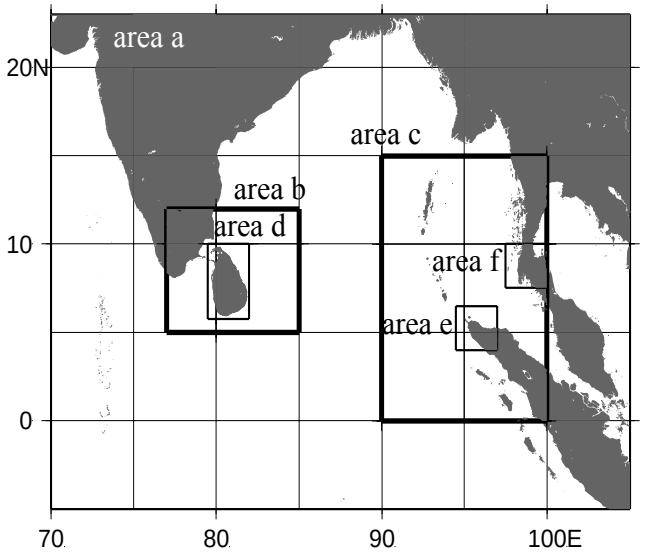

Fig. 4.14 Computation area and nesting system

Table 4.4 Parameters of computation area and nesting system

Area	Grid size	Longitude		Latitude	
a	3 min	70E	105E	5S	23N
b	1 min	77E	85E	5N	12N
c	1 min	90E	100E	0	15
d	20 sec	79.5E	82E	5.75N	10N
e	20 sec	94.5E	97E	4N	6.5N
f	20 sec	97.5E	100E	7.5N	10N

4.3.2 Tsunami Source Model

For the present numerical simulations, the initial fault displacement was inferred from one of the two Harvard CMT solutions (Table 4.5). Two fault models assumed to cover distribution of aftershocks, and these sizes are similar, 500km x 200km. The resulting sea floor deformation was computed by the theoretical method (Mansinha and Smylie, 1971) (Fig. 4.15). Then crustal rigidity is 4×10^{-11} dyne/cm^2. In the numerical computation, dynamic fault parameters are considered. That is, sea bottom deformation starts at the point of main shock, and radiates at rates of rupture velocity of 2.5km/s. Rise time at each point is 0.1 of a second. Time for crustal deformation is about 400 seconds, because the length of the whole fault area is larger than 1000km.

Table 4.5 Fault parameters

	south	north
L(km)	500	500
W(km)	200	200
depth(km)	28.6	28.6
Strike	329	360
Dip	8	8
Slip	110	110
Dislocation(m)	5.0	5.0
Mo(dyne cm)	4.0×10^{29}	

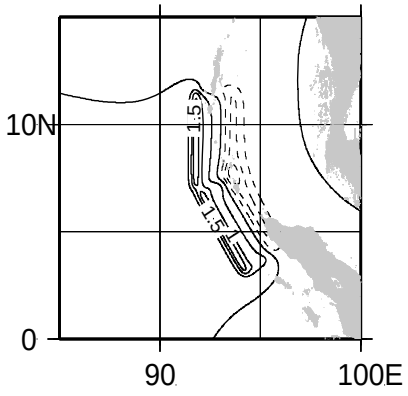

Fig. 4.15 Sea bottom deformation, gap among contour lines is 0.5m.

4.3.3 Results of numerical simulation

Fig. 4.16 shows distributions of measured and calculated tsunami heights along the coast of Thailand. The maximum calculated height on Phuket Island is about 6m and similar to the measured height. On Khao Lak, the maximum calculated height is about 8m, and the measured height was a little larger, which ranges from 9 to 10m. However calculated result describe the difference between heights in Phuket and at Khao Lak, as shown in measured distribution. Therefore both results are harmonious, and this indicates total energy of two fault models is acceptable for tsunami heights in Thailand.

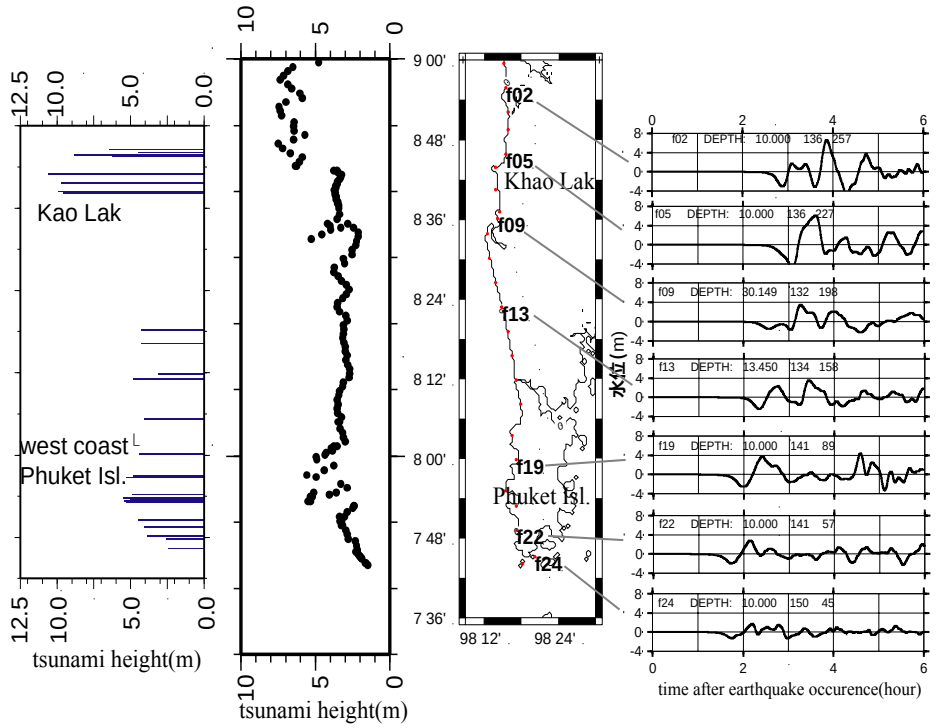

(a)measured result (b)calculated result (c)time series output

Fig. 4.16 Comparison between calculated and measured tsunami height distributions in Thailand, and time series output by calculation along shore

Fig. 4.16 also shows time series output along the coast of Thailand. The tsunami arrived at the southern part of Phuket Island at first. It took 90 minutes to propagate from the tsunami source. Water surface descended first and ascended after half an hour. The tsunami arrival ran to the north direction along the coast of Thailand. Witnesses confirm this feature of the tsunami arrival time. The tsunami arrival time at Khao Lak was an hour later than on Phuket Island. The maximum height was recorded by the second or later ascent wave at four points. Especially maximum height at f19 appeared four and a half hours after the earthquake.

Fig. 4.17 shows distributions of measured and calculated tsunami heights on Sumatra Island. Along the northern coast of Banda Ache, tsunami height by calculation was a maximum of 4m and decreased farther to the west. Calculated heights ranges from 40 % to 50% of measured ones. Along the western coast of northern Sumatra, the tsunami height maximum was 10m, and about 5m at the same coast region of measurement. Measured heights are much larger than calculated ones. The reason for the difference between

calculated and measured results is uniformity of two assumed fault models. That is, real fault movement has plural asperities, and it caused a giant tsunami, which hit to the west coast of northern Sumatra Island.

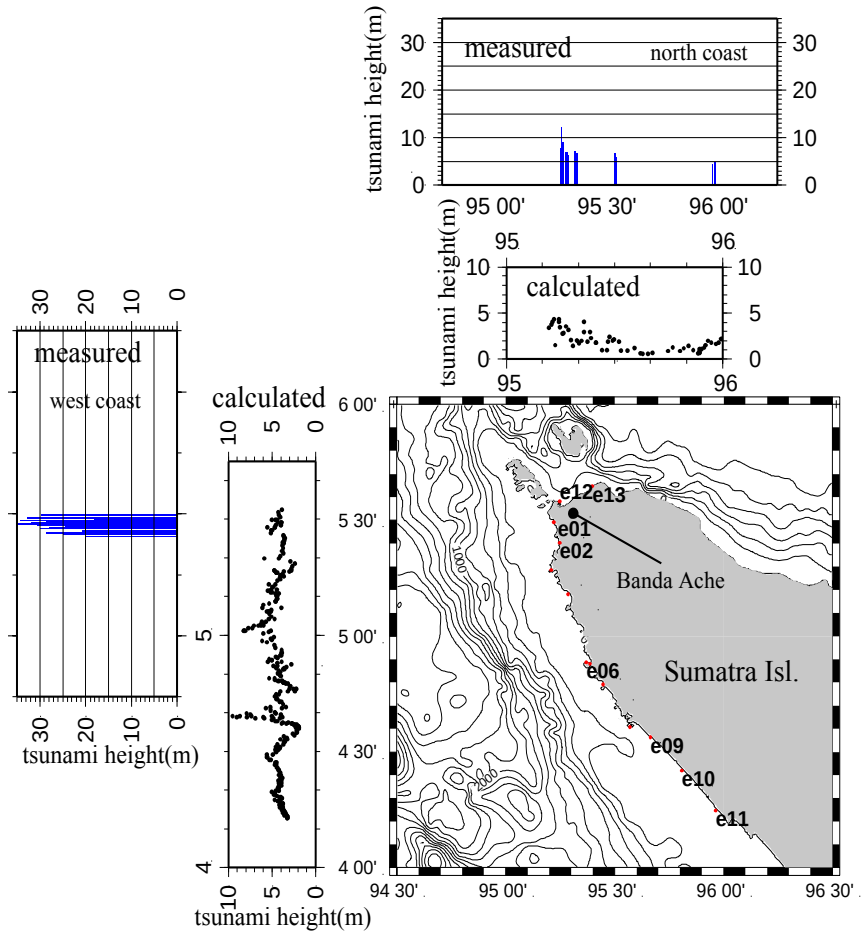

Fig. 4.17 Comparison between calculated and measured tsunami heights distributions in northern Sumatra.

These results of tsunami heights in Thailand and northern Sumatra Island indicate as follows:

1) There are plural asperities on the fault planes.

2) Uniformity in the tsunami source created a giant tsunami the hit northern Sumatra.

3) However it has no effect on the coast at a distance of more than 500km.

References

Asian Tsunami Video.com : Amateur Asian Tsunami Video Footage, http://www.asiantsunamivideos.com/, referred on June 1, 2005

Abe, K. : Revised Mt and run-up estimate for the Indian Ocean Tsunami, e-mail to ITIC Tsunami Bulletin Board posted on January 26, 2005.

BBC : bbc.co.uk homepage - Home of the BBC on the Internet, http://news.bbc.co.uk/, referred on February 28, 2005.

Goto, T and Y. Ogawa: Numerical simulation method of tsunami propagation with the staggered leap-frog scheme, document of Tohoku Univ., 52p, 1982 (in Japanese).

Imamura, F., T. Nagai, H. Takenaka, and N. Shuto: Computer graphics for the study of transoceanic propagation of tsunamis, proceedings of the 4th Pacific Congress of Marine Science and Technology 90, pp118-123, 1990.

Mansinha, L. and D. E. Smylie: The displacement fields of inclined faults, Bulletin of Seismological Society of America、Vol.61、No.5、1971、pp.1433–1440.

Matsutomi, H., Takahashi, T., Matsuyama, M., Harada, K., Hiraishi, T., Suparatid, S. and Nakusakui, S. : The 2004 Off Sumatra Earthquake Tsunami and Damage at Khao Lak and Phuket Island in Thailand, Annual Journal of Coastal Engineering, JSCE, Vol.52, in printing, 2005.

Royal Thai Navy : http://www.navy.mi.th/hydro/tsunami.htm, referred on June 1, 2005.

Sandwell, D. T. and Smith, W. H. F.: Marine gravity anomaly from Geosat and ERS-1 satellite altimetry. J. Geophys, Res., vol.102, pp10039-10050, 1997.

Suzuka, A., Takahashi and T., Matsutomi, H. : Numerical simulation on the Sumatra earthquake tsunami along the southwest coast of Thailand, Annual Journal of Coastal Engineering, JSCE, Vol.52, in printing, 2005.

USGS : Largest Earthquakes in the world, http://neic.usgs.gov/neis/eqlists/10maps_world.html, referred on June 1, 2005.

Utsu, T. : Seismology, 376 p., Kyoritsu Shuppan, 2001.

Yamanaka, Y. : EIC Seismological Note No. 161+, http://www.eri.u-tokyo.ac.jp/sanchu/Seismo_Note/2004/EIC161a.html, referred on June 1, 2005.